

Influence of hydrodynamics on the interpretation of the high p_T hadron suppression at RHIC

T. Peitzmann¹

Utrecht University, NL-3508 TA Utrecht, The Netherlands

Abstract

A hybrid parameterization including contributions of hydrodynamics and of expectations from the spectral shape observed in p+p collisions is introduced. This parameterization can successfully describe identified hadron spectra over a wide range of p_T in Au+Au reactions at $\sqrt{s_{NN}} = 200$ GeV for all centralities. The parameters of the hydrodynamic source compare reasonably well to other attempts to describe the spectra. The description is obtained using one universal suppression factor of the hard scattering component independent of p_T and hadron species. For the fit results obtained the observed nuclear modification factor for the different particles converges to a universal suppression behavior for $p_T > 6$ GeV/c.

Key words: ultrarelativistic heavy-ion collisions, hadron production, hydrodynamics, hard scattering, jet quenching

PACS: 25.75.Dw

1 Introduction

One of the most interesting recent observations in ultrarelativistic heavy-ion physics was the suppressed yield of moderately high p_T neutral pions in central Au+Au collisions at $\sqrt{s_{NN}} = 130$ GeV with respect to appropriately scaled p+p results [1], in contrast to a strong enhancement observed at lower beam energies [2]. This was qualitatively supported by the observation of a suppression in non-identified charged hadron yields [1,3]. Among the theoretical studies on the origin of the observed high p_T deficit [4,5,6,7,8,9], most are based on the early prediction [10] of the so-called jet quenching, i.e. the energy loss

¹ email: t.peitzmann@phys.uu.nl

of fast partons induced by a hot and dense quark-gluon-plasma. Others invoke initial state parton saturation [8] or final state hadronic interactions [9]. While these different scenarios are being discussed, the interpretation is complicated by the parallel observation of a comparably large proton and antiproton yield at intermediate momenta [11], which are apparently not similarly suppressed. These observations have been confirmed by the new measurements at $\sqrt{s_{NN}} = 200$ GeV [12,13], which extend out to considerably higher transverse momenta for the pion measurement.

Simultaneously, there are a number of hints from the RHIC experiments that equilibration may be achieved already in an early state and that the behavior of the system might at least partly be described by hydrodynamics, most notably the observation of strong elliptic flow [14,15]. Also the hadron momentum spectra can be described by hydrodynamic calculations and parameterizations quite well in the low and intermediate momentum range [16,17,18,19]. In particular, the large (anti)proton/pion ratio can easily be explained by such calculations. While at very high p_T the influence of hydrodynamic production should become negligible, in the intermediate momentum range there will be a smooth transition from hydrodynamic behavior to hard scattering. It is therefore of interest to study the implications of hydrodynamic particle production for the interpretation of the pion suppression.

In the present paper I will attempt to describe hadron spectra with a parameterization combining hydrodynamic components and components similar to the original particle production in p+p collisions. This is considered a simple approximation to the more complicated real situation in heavy ion collisions, where, even if hydrodynamics is relevant for a large fraction of the particle spectra, there will always be some non-equilibrium contribution e.g. from the surface of the collision zone. In reality, part of this would likely be intermediate in shape between true p+p spectra and hydrodynamics, but it is beyond the scope of this paper to attempt to describe the full non-equilibrium nature of these collisions. The calculations should nevertheless provide a better understanding of the hadron spectra than pure hydrodynamic calculations. Furthermore, the inclusion of an explicit hard component will allow to describe the spectra out to high p_T .

2 The model

2.1 *The hydrodynamical parameterization*

The present paper uses an extension of the hydrodynamical parameterization of [16], which includes effects of transverse flow and resonance decays. It was

originally based on a computer program by Wiedemann and Heinz [20], which in turn builds upon [21]. It parameterizes the particle source at freeze-out as:

$$\begin{aligned} \frac{dN_r^{\text{dir}}}{dY dM_T^2} &= N_{\text{hydro}} \cdot \text{MeV}^{-3} \cdot (2J_r + 1) \\ &\times M_T \int_0^4 \xi d\xi \frac{1}{1 + \exp \Delta(\xi - 1)} K_1 \left(\frac{M_T}{T_{\text{kin}}} \cosh \eta_t(\xi) \right) \\ &\times I_0 \left(\frac{P_T}{T_{\text{kin}}} \sinh \eta_t(\xi) \right). \end{aligned} \quad (1)$$

The integral over ξ contains a Woods-Saxon spatial profile with a diffuseness parameter Δ and the two Bessel functions which originate from the boost of a thermal distribution with a transverse collective velocity. The transverse expansion is described by a transverse rapidity, which is parameterized as $\eta_t(\xi) = \eta_f \cdot \xi$, i.e. depending linearly on the normalized radial coordinate $\xi = r/R$. I fix $\Delta \equiv 50$ which yields a nearly box-like spatial shape of the source, as this has been shown to be a reasonable assumption [22,23,16]. A fixed upper limit ($\xi = 4$) has to be chosen for the numerical integration, for the distribution used in this work this is effectively equivalent to setting the upper limit to infinity. A spin degeneracy factor is included, and there is an additional arbitrary normalization factor N_{hydro} , which is the same for all particle species and controls the relative strength of the hydrodynamical component. While the spectral shape is a.o. determined by the kinetic temperature T_{kin} , the normalization for each particle species is readjusted to the chemical temperature T_{chem} assuming that dN/dy at midrapidity scales with the temperature as [21]:

$$\frac{dn_{\text{th}}}{dy} = \frac{V}{(2\pi)^2} T^3 \left(\frac{m^2}{T^2} + \frac{2m}{T} + 2 \right) \exp \left(-\frac{m}{T} \right). \quad (2)$$

The parameterization attempts to describe the production of pions, protons and antiprotons and kaons; it includes contributions from the following resonances: ρ , K_S^0 , K^* , Δ , $\Sigma + \Lambda$, η , ω , η' . For the description of baryons a baryonic chemical potential μ_B is used, while for strange particles an additional strangeness suppression factor λ_s is introduced. For each hadron species the spectrum of hydrodynamically produced particles $f_{\text{hydro}}^{(X)}(p_T)$ is given as the sum of the direct contribution and those of the appropriate resonances:

$$\begin{aligned} f_{\text{hydro}}^{(X)}(p_T) &= \frac{dN_X^{\text{dir}}}{dY dM_T^2} + \\ &+ \sum_r \int_{\text{phase space}} dW^2 dY_r dM_{Tr} \cdot F(W, P_r, p) \cdot \frac{dN_r^{\text{dir}}}{dY_r dM_{Tr}^2}, \end{aligned} \quad (3)$$

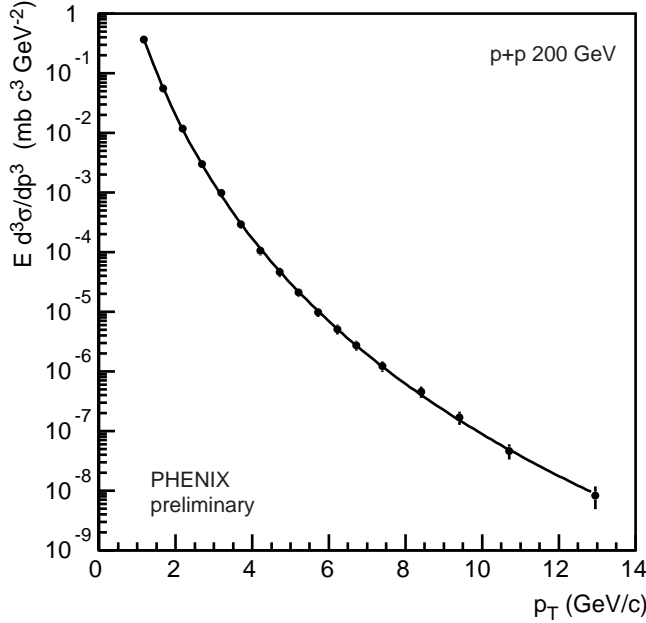


Fig. 1. Transverse momentum spectrum of neutral pions in p+p collisions at $\sqrt{s} = 200$ GeV as measured by the PHENIX experiment [25]. The solid line shows a fit of equation 4.

where W is the invariant mass, Y_r the rapidity and M_{Tr} the transverse mass of the resonance, and $F(W, P_r, p)$ is the appropriate phase space factor.

2.2 The p+p parameterization

As suggested by Hagedorn [24], hadron spectra in high energy p+p collisions can be described by a QCD-inspired power law with exponential continuation at lower momenta. Such a spectral shape can be written as:

$$f(p_T) = \begin{cases} C \left(\frac{nT - p_{T1}}{nT} \right)^n \exp \left(\frac{p_{T1} - p_T}{T} \right) & : p_T \leq p_{T1} \\ C \left(\frac{nT - p_{T1}}{nT - p_{T1} + p_T} \right)^n & : p_T > p_{T1}. \end{cases} \quad (4)$$

Here n and T are adjustable parameters. T is related to the more frequently used parameter p_0 by: $p_0 = nT - p_{T1}$. Fig. 1 shows a fit of this function to the neutral pion spectrum measured in p+p collisions by the PHENIX experiment [25]. $p_{T1} = 1$ GeV/c was chosen. The function provides a perfect fit over the full range of the measured data. As fit parameters $C = 280.52$ mbGeV $^{-2}$, $T = 0.226$ GeV and $n = 9.89$ have been obtained.

These distributions contain a component due to hard scattering processes, which is expected to lead to a power law shape dominating at high p_T . At

low p_T production from string fragmentation, a soft process, will be much more abundant and therefore dominate there. For the later description of spectra in heavy-ion reactions I will attempt to separate the two components, although a clear separation directly from the spectra is not possible. However, the exponential shape at low p_T is believed to be due to the soft component, while at very high p_T the shape will turn into a pure power law $\propto p_T^{-n}$. The separation is of course completely arbitrary when looking at the fit to the data in Fig. 1 alone. In fact, there the exponential is not even fitted directly to the data and is only determined as the differentiable continuation of the shape at higher p_T . The value of the separation point $p_{T1} = 1 \text{ GeV}/c$ is not uniquely determined, but it yields a reasonable inverse slope parameter for the exponential.

The separation is necessary for a comparison to heavy ion collisions, because the different physical origin of the two components will lead to different scaling behavior, as the number of hard collisions increases more rapidly with increasing mass of the nuclei than the number of strings, i.e. the number of participant pairs. I will assume the soft contribution to be described by the exponential:

$$s(p_T) = C_s \left(\frac{nT - p_{T1}}{nT} \right)^n \exp \left(\frac{p_{T1} - p_T}{T} \right) \quad (5)$$

After subtraction of this part the hard component can be written as:

$$h(p_T) = \begin{cases} 0 & : p_T \leq p_{T1} \\ C_h \left[\left(\frac{nT - p_{T1}}{nT - p_{T1} + p_T} \right)^n - \left(\frac{nT - p_{T1}}{nT} \right)^n \exp \left(\frac{p_{T1} - p_T}{T} \right) \right] & : p_T > p_{T1}, \end{cases} \quad (6)$$

where $C_s = C_h = C$ for p+p collisions.

This parameterization with a subtracted exponential may look artificial. One should remember, however, that already the original *power-law-like* shape suggested by Hagedorn was an effective parameterization which turns into a power law for very high p_T . The deviation from the power law at lower momenta, also to be seen as a variation of the exponent with momentum, was not derived from underlying principles, but chosen to describe the experimental data. The hard component introduced here is equivalent at high p_T and takes into account partial contributions of a soft component at intermediate p_T .

The pion spectrum is:

$$f_{pp}^{(\pi)}(p_T) = s(p_T) + h(p_T). \quad (7)$$

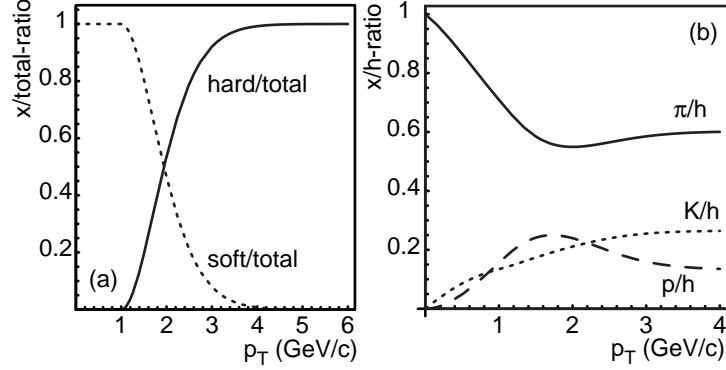


Fig. 2. a) Assumed relative contribution of the soft and hard components of the pion spectrum in $p+p$. b) Fraction of the total number of charged hadrons belonging to different hadron species. The solid line represents the pion fraction, the dotted line the kaons and the dashed line the protons and antiprotons.

This is essentially only a rewriting of equation 4. The main purpose of this separation is the possibility to scale the two components independently when increasing the system size by going to heavy-ion collisions. In naïve pictures of particle production the hard component is expected to increase with the number of nucleon-nucleon collisions, as cross sections are small and processes are incoherent. The soft component, however, will more likely scale with the number of participating nucleons as suggested by the wounded nucleon model. The prescription used here leads to a continuous transition between the soft and hard component as can be seen in Fig. 2a. The two components are of similar magnitude for $p_T \approx 2 \text{ GeV}/c$.

To describe the spectra of other hadron species further assumptions are necessary. The only data from similar beam energies and a reasonably large coverage in p_T are available from the ISR [26]. One of the major observations in this paper was, that the p_T -dependent ratios of different hadron species were to a good approximation independent of the beam energy studied. The kaon, proton and antiproton spectra have thus been tuned to reproduce the observed ratios. This has been achieved by using for kaons:

$$f_{pp}^{(K)}(p_T) = 0.44 \cdot \tanh(0.46 \text{ GeV}^{-1} c p_T) \cdot s(p_T) + 0.44 \cdot h(p_T), \quad (8)$$

for protons:

$$f_{pp}^{(p)}(p_T) = \frac{1.8 \cdot \tanh(0.25 \text{ GeV}^{-2} c^2 p_T^2)}{1.3 + 0.4 \text{ GeV}^{-1} c p_T} \cdot s(p_T) + 0.33 \cdot h(p_T), \quad (9)$$

and for antiprotons:

$$f_{pp}^{(\bar{p})}(p_T) = \frac{1.8(0.3 + 0.4 \text{ GeV}^{-1} c p_T) \cdot \tanh(0.25 \text{ GeV}^{-2} c^2 p_T^2)}{1.3 + 0.4 \text{ GeV}^{-1} c p_T} \cdot s(p_T) + 0.11 \cdot h(p_T). \quad (10)$$

The analytic expressions have been chosen because they can conveniently describe the shapes observed experimentally, they have no physical significance. The parameters have been tuned to describe the experimentally observed ratios obtained at the ISR (see Fig. 14 in [26]). They lead to particle ratios as shown in Fig. 2b. No error analysis has been done for the parameters used in equations 8, 9 and 10. Consequently the related additional uncertainty in the final fits has not been taken into account.

3 Fits to experimental spectra

Fits of the function

$$f^{(X)}(p_T) = f_{hydro}^{(X)} + f_{pp}^{(X)} \quad (11)$$

have been performed to spectra of identified hadrons as measured by the PHENIX experiment in Au+Au collisions at 200 GeV. Preliminary spectra of charged pions, kaons, protons and antiprotons [27] and neutral pions [28] have been used simultaneously for a given centrality. The centrality classes used are summarized in Table 1 together with estimates of the number of binary

Table 1

Average number of NN collisions and participant nucleons for centrality classes as used by PHENIX [29].

Centrality bin	$\langle N_{coll} \rangle$	$\langle N_{part} \rangle$
0-5%	1065.4 ± 105.3	351.4 ± 2.9
5-10%	845.4 ± 82.1	299.0 ± 3.8
10-15%	672.4 ± 66.8	253.9 ± 4.3
15-20%	532.7 ± 52.1	215.3 ± 5.3
20-30%	373.8 ± 39.6	166.6 ± 5.4
30-40%	219.8 ± 22.6	114.2 ± 4.4
40-50%	120.3 ± 13.7	74.4 ± 3.8
50-60%	61.0 ± 9.9	45.5 ± 3.3
60-70%	28.5 ± 7.6	25.7 ± 3.8
70-80%	12.4 ± 4.2	13.4 ± 3.0

collisions $< N_{coll} >$ and the number of participants $< N_{part} >$ [29]. Besides the parameters of the hydrodynamical parameterization two normalization parameters $N_s = C_s/C$ and $N_h = C_h/C$ of the pp parameterization enter. All parameters are summarized in Table 2. Four different sets of fits have been performed:

- (1) Pure hydrodynamic fits (i.e. $N_s = N_h = 0$) using only data for $m_T - m_0 \leq 1 \text{ GeV}/c^2$.
- (2) Pure hydrodynamics ($N_s = N_h = 0$) using the full data sets.
- (3) Pure fits of the pp parameterization ($N_{hydro} = 0$) using the full data sets.
- (4) Fits of the full hybrid parameterization using the full data sets.

The hydrodynamic fits (1) to the low momentum region provide excellent fits for all centralities. There is some ambiguity in the choice of T_{kin} and $\langle \beta_T \rangle$ – to some extent a large velocity can be compensated by a small temperature, and vice versa. To avoid these ambiguities all later fits have been performed with setting $T_{kin} \equiv 120 \text{ MeV}$, which provides good agreement at low m_T for all centralities. One should note that while especially the flow velocity depends on the choice of the freeze-out temperature, the results on the scaling of the different particle species as discussed below are not strongly affected.

Table 2

Fit parameters of the proposed parameterization. Note, that while the average velocity is given here, this has been calculated from the transverse rapidity parameter η_f which was used in the fits. Fit parameter values for central collisions with their fit errors are stated in the right column.

parameter	remark	fit results (central)
N_{hydro}	normalization of hydrodynamical contribution	7.7 ± 3.1
T_{kin}	kinetic temperature	120 MeV
$\langle \beta_T \rangle$	average transverse expansion velocity	0.529 ± 0.015
T_{chem}	chemical temperature	$160.8 \pm 4.3 \text{ MeV}$
μ_B/T_{chem}	baryonic chemical potential	0.17 ± 0.03
λ_s	strangeness suppression	0.96 ± 0.15
N_s	normalization of soft component	124 ± 100
N_h	normalization of hard component	173 ± 20

Examples of these fits to the spectra from peripheral collisions (70 – 80%) are shown in Fig. 3. The pion spectra can be well described already by the pure pp parameterization as well as the full fit, the pure hydrodynamics fit, however, fails to describe the high m_T tail. While for pions all parameterizations provide a good description at lower m_T , for kaons, proton and antiprotons discrepancies are seen mostly at low momenta. These discrepancies are largest

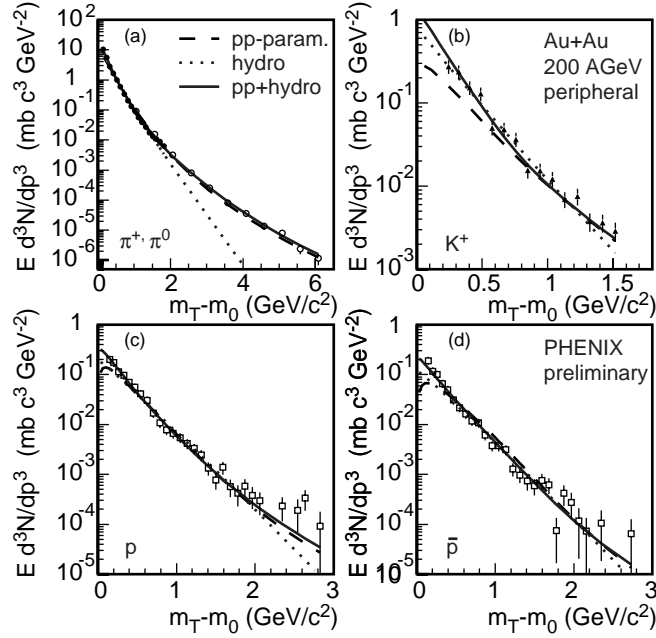


Fig. 3. Transverse momentum spectrum of pions, kaons, protons and antiprotons in peripheral Au+Au collisions (70 – 80%) at $\sqrt{s} = 200$ GeV as measured by the PHENIX experiment [27,28]. The dotted line shows pure hydrodynamics fits (2), the dashed line a fit of the pure pp parameterization (3) and the solid line shows a full fit (4) of equation 11.

for the pp parameterization. As I am most interested in the behavior at high momenta, this will not be investigated further. One may take it as a hint that low momentum particle ratios extracted from pp measurements at ISR [26] do not completely describe even peripheral heavy ion collisions at RHIC, while the spectral shape of pions appears to be well described over the range investigated here. The reasonable description of all particle species at intermediate m_T lends some support to the choice of the pp parameterization. The full fit combining hydrodynamics and the pp parameterization provides an excellent description of all spectra. Of course, the high momentum behavior of the heavier particles can not be thoroughly tested from the limited momentum range alone.

Similarly, Fig. 4 shows fits to spectra for central collisions (0 – 5%). Again, it can be seen that hydrodynamics alone fails to describe the tail of the pion spectra, while the other parameterizations do a reasonably good job. However, for the heavier particles the failure of the pure pp parameterization is obvious. There are large discrepancies for the kaons over the whole momentum range and for protons and antiprotons for large momenta. It is clear that the spectra for central collisions can not be described neither by hydrodynamics nor a pure pp parameterization alone, however the combination of both provides again an excellent description. An equally good description can be obtained with this parameterization for all centralities.

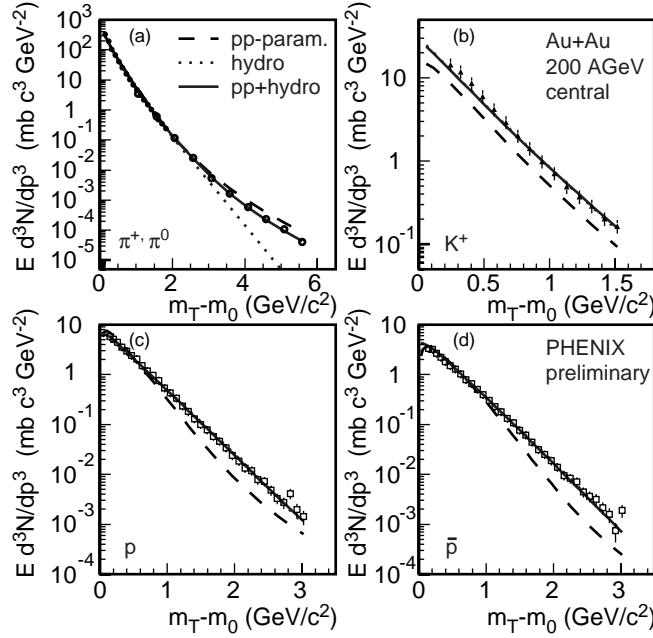


Fig. 4. Transverse momentum spectrum of pions, kaons, protons and antiprotons in central Au+Au collisions (0 – 5%) at $\sqrt{s} = 200$ GeV as measured by the PHENIX experiment [27,28]. The dotted line shows pure hydrodynamics fits (2), the dashed line a fit of the pure pp parameterization (3) and the solid line shows a full fit (4) of equation 11.

4 Discussion

Although the description of spectra by means of hydrodynamic parameterizations is not the ultimate aim of this paper, it is still instructive to study the behavior of the fit parameters for the different centralities. Fig. 5 shows parameter values for different fits as a function of centrality. The open symbols show results from pure hydrodynamic fits. Those have been performed for lower m_T only with the kinetic temperature being either fixed to $T_{kin} = 120$ or 140 MeV or varying freely, in addition a fit with unconstrained T_{kin} has been performed to the full available m_T range. The filled circles show the same parameters for a full fit of equation 11 including the soft and hard components and assuming $T_{kin} = 120$ MeV. It is noteworthy that all these fits show essentially very similar results. The chemical temperature (Fig. 5a) is $T_{chem} \approx 160$ MeV for all centralities, also the baryonic chemical potential (b) appears to be almost independent of centrality with a value of $\mu_B/T_{chem} \approx 0.15 - 0.2$. The strangeness suppression (c) is strongest for peripheral collisions with $\lambda_s \approx 0.65$ increasing to $\lambda_s \approx 0.9$ for central collisions. The transverse flow velocity also increases considerably with centrality from $\langle \beta_T \rangle \approx 0.25$ for peripheral reactions to $\langle \beta_T \rangle \approx 0.5$ in central reactions. The chemical temperature appears to be similar, but slightly smaller than values obtained for central collisions of Au+Au at 130 GeV [16,30]. Kinetic temperature and flow velocity are similar

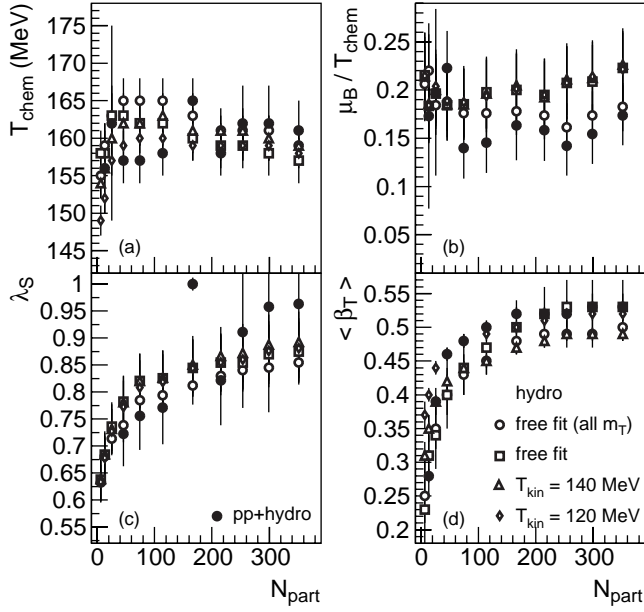


Fig. 5. Parameters of the hydrodynamical component of fits to Au+Au collisions at $\sqrt{s} = 200$ GeV as a function of the number of participants. a) chemical temperature, b) baryonic chemical potential normalized to the chemical temperature, c) strangeness suppression factor, d) average transverse expansion velocity. The open symbols show the results from pure hydrodynamic fits under different conditions, the filled circles show results using the full parameterization.

to values obtained in [16] for 130 GeV or in [18] for 200 GeV, when considering that the latter analysis did not take the influence of resonances into account. The results of the hydrodynamical parameters obtained here are therefore not at all extraordinary or astonishing. (For reference the fit values for central collisions using the full fit are also given in Table 2.)

Already in [16] it was argued that the hydrodynamic contribution to the hadron yield even beyond $p_T = 3$ GeV/ c is not negligible. This question can be revisited with the help of the refined fits performed here. Fig. 6 shows the relative contributions of the hydrodynamical component to the full fits for central collisions. Again, it can be seen that this contribution is significant for pions beyond $p_T = 3$ GeV/ c . Moreover, the importance of this contributions reaches out to even higher p_T for the heavier particles, as is expected for a hydrodynamic source.² This hydrodynamic component causes very naturally a different behavior of the particle ratios compared to p+p collisions. The proton/pion and antiproton/pion ratios (as displayed in Fig. 7a) show pronounced maxima close to a value of 1 between p_T of 2 and 4 GeV/ c . Consequently there is a strong minimum in the pion/hadron ratio (see Fig. 7b).

² The strong increase of the relative importance of the hydrodynamic contribution in protons and antiprotons at low p_T is due to the suppression of these particles in the non-hydro production (see Fig. 2).

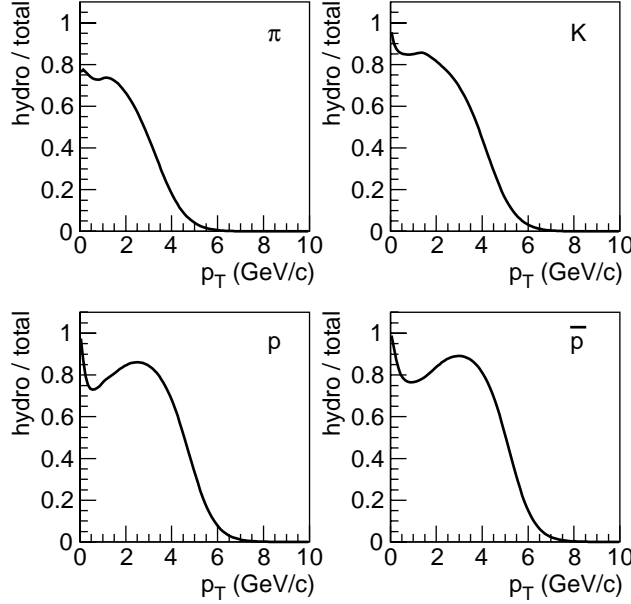


Fig. 6. Ratio of the hydrodynamical contribution to the total spectrum in central Au+Au collisions at $\sqrt{s} = 200$ GeV as a function of p_T . The ratios for pions, kaons, protons and antiprotons are shown separately.

The kaon/hadron ratio rises much faster than in p+p.

This will also influence the comparison of spectra from central nuclear collisions to those from p+p collisions as is customary in the investigations of high p_T hadron suppression. One uses the *nuclear modification factor*:

$$R_{AA}^X(p_T) = \frac{(1/N_{AA}^{evt}) d^2N_{AA}^X/dydp_T}{\langle N_{coll} \rangle (1/N_{pp}^{evt}) d^2N_{pp}^X/dydp_T}. \quad (12)$$

This can easily be calculated from the parameterization used here. Fig. 8 shows R_{AA} for the different hadron species. R_{AA} for pions decreases from about 0.4

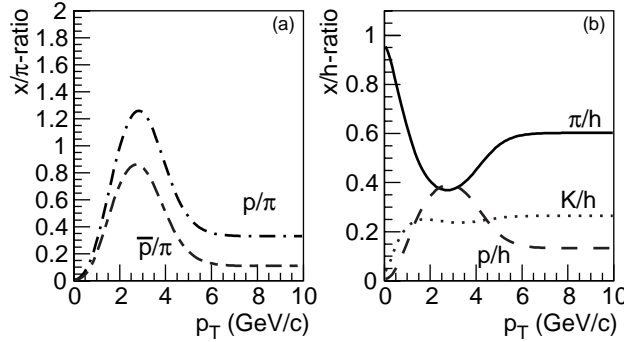


Fig. 7. Hadron ratios in central Au+Au collisions at $\sqrt{s} = 200$ GeV as a function of p_T . a) Protons/pions and antiprotons/pions, b) charged pions/charged hadrons, charged kaons/charged hadrons and proton+antiprotons/charged hadrons.

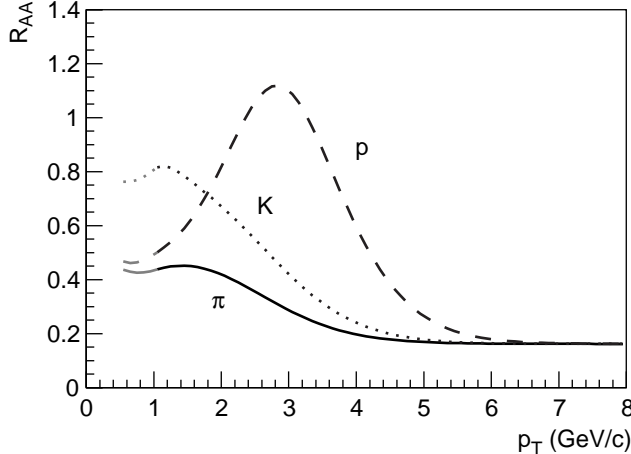


Fig. 8. Nuclear modification factor (equation 12) as a function of p_T for pions, kaons and protons+antiprotons.

at 2 GeV/c to 0.2 at high p_T . For heavier particles R_{AA} starts out at higher values and reaches the same asymptotic value more slowly. For protons and antiprotons there is a peak structure with a small enhancement ($R_{AA} > 1$) in the intermediate p_T range.

Finally one can investigate the relative strength of the soft and especially the hard component, N_s and N_h as a function of centrality. Fig. 9a shows $N_s/(0.5 \times N_{part})$ as a function of N_{part} . Without taking into account any hydrodynamic production this normalized strength of the soft contribution increases significantly with increasing centrality, while for the full parameterization the ratio stays close or below a value of 1. The difference between the two estimates may just be seen as the importance of the added hydrodynamic contribution, which very naturally appears to be negligible for the most peripheral collisions and increases strongly with centrality. A similar difference is seen when normalizing to N_{coll} (Fig. 9b), however, now all values are smaller than 1. Even more interesting is the evolution of the hard component. Fig. 9d shows N_h/N_{coll} as a function of N_{part} . This can effectively be seen as an average value of R_{AA} over the p_T range of the hard component. Qualitatively the trend of both parameterizations is similar, there are, however, significant quantitative differences. For the pure pp parameterization the apparent average suppression changes from 0.8 for peripheral to 0.4 for central reactions. When accounting for the hydrodynamic contribution, the ratio changes more drastically from no suppression (= 1) to a value of 0.2. Within this model, these are the true suppression values of the hard component independent of species and p_T .

The normalizations of the soft and hard component are well defined from their fit to pp data, the hydrodynamic component has an overall arbitrary normalization related e.g. to the unknown source volume. Once the normalization is

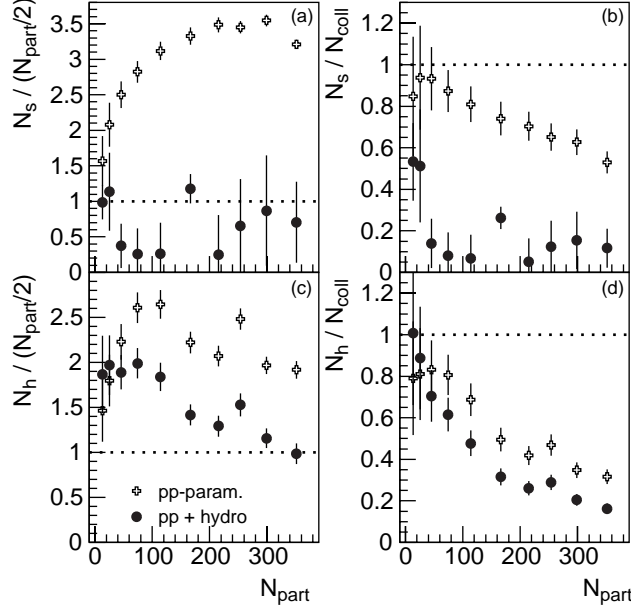


Fig. 9. Strength of the soft and hard component as a function of the number of participants. The open crosses show the pure pp parameterization, the filled circles the full fit including the pp parameterization and hydrodynamic contributions. a) $N_s/(0.5 * N_{part}/2)$, b) N_s/N_{coll} , c) $N_h/(0.5 * N_{part}/2)$, d) N_h/N_{coll}

fixed for a given centrality, it is still instructive to compare it to those for other centralities. Fig. 10 shows N_{hydro}/N_{part} normalized to one for the most central collisions as a function of the the number of participants. While N_{part} varies by a factor of almost 30 over the centrality range investigated, the ratio appears to be constant within errors, i.e. the size of the hydrodynamic system is to a large extent determined from the collision geometry. This is another hint for the consistency of the model used. Within this parameterization one can deal simultaneously with a suppression of the hard scattering component and a build up of hydrodynamic behavior. It would of course be of great interest to study explicitly the dynamics of the interactions between jets and the hydrodynamic system as e.g. performed in [31] - this is however far beyond the scope of this paper.

5 Summary

Fits of a hybrid parameterization containing both hydrodynamics and elementary soft and hard contributions to hadron spectra measured in Au+Au collisions at $\sqrt{s_{NN}} = 200$ GeV [27,28] have been performed. The input distributions have been tuned to describe the spectra of neutral pions in p+p collisions at $\sqrt{s} = 200$ GeV [25] and the particle ratios as measured at the ISR [26]. Keeping the parameters of the hydrodynamic source and the relative

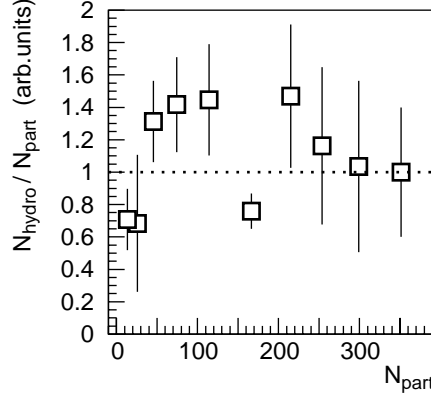


Fig. 10. Strength of the hydrodynamic component per participant as a function of the number of participants. The ratio is normalized to one for the most central collisions (see Table 2).

normalizations of the soft and hard components as free parameters an excellent description of hadron spectra for all centralities can be obtained. The parameters obtained for the hydrodynamic source are reasonable: The chemical temperature of $T_{chem} \approx 160$ MeV and the baryonic chemical potential of $\mu_B/T_{chem} \approx 0.15 - 0.2$ are almost independent of centrality. For peripheral collisions the strangeness suppression factor is $\lambda_s \approx 0.65$ and the flow velocity is $\langle \beta_T \rangle \approx 0.25$, while for central collisions I obtain $\lambda_s \approx 0.9$ and $\langle \beta_T \rangle \approx 0.5$.

The hydrodynamic source contributes a significant fraction of hadrons at intermediate p_T reaching out to at least $p_T = 3$ GeV/ c for pions and $p_T = 5$ GeV/ c for protons and antiprotons, thereby explaining the large baryon-to-pion ratio in central Au+Au collisions. It also results in a very different scaling behavior for the different species, even if one assumes one universal suppression factor of the hard component for all particle species. The suppression would only be visible for proton and antiprotons for $p_T > 4$ GeV/ c . The universal suppression factor extracted is smaller than 0.2 for central collisions, the merging of R_{AA} for different species can be seen for $p_T > 6$ GeV/ c .

References

- [1] PHENIX collaboration, K. Adcox et al., Phys. Rev. Lett. **88** (2002) 022301.
- [2] WA98 collaboration, M.M. Aggarwal et al., Eur. Phys. J. C **23** (2002) 225.
- [3] STAR collaboration, C. Adler et al., Phys. Rev. Lett. **89** (2002) 202301.
- [4] I. Vitev and M. Gyulassy, Phys. Rev. Lett. **89** (2002) 252301.
- [5] S. Jeon, J. Jalilian-Marian and I. Sarcevic, Nucl. Phys. A **715** (2003) 795c-798c.

- [6] G.G. Barnafoldi, P. Levai, G. Papp, G. Fai, Y. Zhang, nucl-th/0212111; V. Greco, C.M. Ko and P. Levai, Phys. Rev. Lett. **90** (2003) 202302.
- [7] X. N. Wang, Nucl. Phys. A **715** (2003) 775c-778c.
- [8] D. Kharzeev, E. Levin and L. McLerran, Phys. Lett. B **561** (2003) 93-101.
- [9] K. Gallmeister, C. Greiner and Z. Xu, Phys. Rev C **67** (2003) 044905; nucl-th/0202051.
- [10] M. Gyulassy and M. Plümer, Phys. Lett. B **243** (1990) 432; X.N. Wang and M. Gyulassy, Phys. Rev. Lett. **68** (1992) 1480.
- [11] PHENIX collaboration, K. Adcox et al., Phys.Rev.Lett. **88** (2002) 242301.
- [12] PHENIX collaboration, S. Mioduszewski et al., Nucl. Phys. A **715** (2003) 199c-208c.
- [13] STAR collaboration, G.J. Kunde et al., Nucl. Phys. A **715** (2003) 189c-198c.
- [14] STAR collaboration, K.H. Ackermann et al., Phys.Rev.Lett. **86** (2001) 402-407; C. Adler et al., Phys.Rev.Lett. **87** (2001) 182301.
- [15] PHENIX collaboration, K. Adcox et al., Phys.Rev.Lett. **89** (2002) 212301.
- [16] T. Peitzmann, Eur. Phys. J. C **26** (2003) 539.
- [17] W. Broniowski and W. Florkowski, Phys.Rev.Lett. **87** (2001) 272302.
- [18] PHENIX collaboration, J.M. Burward-Hoy et al., Nucl. Phys. A **715** (2003) 498c-501c.
- [19] P.F. Kolb and R. Rapp, Phys. Rev. C **67** (2003) 044903.
- [20] U.A. Wiedemann and U. Heinz, Phys. Rev. C **56** (1997) 3265.
- [21] E. Schnedermann, J. Sollfrank, and U. Heinz, Phys. Rev. C **48** (1993) 2462.
- [22] B. Tomasik, U.A. Wiedemann, and U. Heinz, preprint nucl-th/9907096.
- [23] P. Huovinen, P.F. Kolb, U. Heinz, P.V. Ruuskanen, and S.A. Voloshin, Phys. Lett. B **503** (2001) 58-64
- [24] R. Hagedorn, Riv. Nuovo Cim. **6 N10** (1984) 1-50.
- [25] PHENIX collaboration, H. Torii et al., Nucl. Phys. A **715** (2003) 753c-756c.
- [26] B. Alper et al., Nucl. Phys. B **100** (1975) 237.
- [27] PHENIX collaboration, T. Chujo et al., Nucl. Phys. A **715** (2003) 151c-160c.
- [28] PHENIX collaboration, D. d'Enterria et al., Nucl. Phys. A **715** (2003) 749c-752c.
- [29] K. Reygers, private communication.
- [30] P. Braun-Munzinger, D. Magestro, K. Redlich and J. Stachel, Phys. Lett. B **518** (2001) 41-46.
- [31] T. Hirano and Y. Nara, Phys. Rev. C **66** (2002) 041901R.